Topical application of *Porphyromonas gingivalis* into the gingival pocket in mice leads to chronic-active infection, periodontitis and systemic inflammation

SHARON KIM[1*], YASUHIKO BANDO[1*], CHUNGYU CHANG[2], JEONGA KWON[1], BERTA TARVERTI[1], DOOHYUN KIM[1], SUNG HEE LEE[1], HUNG TON-THAT[2,3], REUBEN KIM[1,2], PETER L. NARA[4] and NO-HEE PARK[1,5]

[1]The Shapiro Family Laboratory of Viral Oncology and Aging Research, UCLA School of Dentistry; [2]Section of Oral Biology, UCLA School of Dentistry; [3]Molecular Biology Institute, UCLA, Los Angeles, CA 90095; [4]Keystone Bio Incorporated, Suite 200, St. Louis, MO 63110; [5]Department of Medicine, David Geffen School of Medicine at UCLA, Los Angeles, CA 90095, USA

Received March 2, 2022; Accepted April 14, 2022

DOI: 10.3892/ijmm.2022.5159

Abstract. *Porphyromonas gingivalis (Pg)*, one of the 'red-complex' perio-pathogens known to play a critical role in the development of periodontitis, has been used in various animal models to mimic human bacteria-induced periodontitis. In order to achieve a more realistic animal model of human *Pg* infection, the present study investigated whether repeated small-volume topical applications of *Pg* directly into the gingival pocket can induce local infection, including periodontitis and systemic vascular inflammation in wild-type mice. Freshly cultured *Pg* was topically applied directly into the gingival pocket of the second molars for 5 weeks (3 times/week). After the final application, the mice were left in cages for 4 or 8 weeks and sacrificed. The status of *Pg* colony formation in the pocket, gingival inflammation, alveolar bone loss, the expression levels of pro-inflammatory cytokines in the serum and aorta, the presence of anti-*Pg* lipopolysaccharide (LPS) and gingipain (Kpg and RgpB) antibodies in the serum, as well as the accumulation of *Pg* LPS and gingipain aggregates in the gingiva and arterial wall were evaluated. The topical application of *Pg* into the gingival pocket induced the following local and systemic pathohistological changes in mice when examined at 4 or 8 weeks after the final topical *Pg* application: *Pg* colonization in the majority of gingival pockets; increased gingival pocket depths; gingival inflammation indicated by the increased expression of TNF-α, IL-6 and IL-1β; significant loss of alveolar bone at the sites of topical *Pg* application; and increased levels of pro-inflammatory cytokines, such as TNF-α, IL-1β, IL-17, IL-13, KC and IFN-γ in the serum in comparison to those from mice receiving PBS. In addition, the *Pg* application/colonization model induced anti-*Pg* LPS and gingipain antibodies in serum, as well as the accumulation of *Pg* LPS and gingipain aggregates in the gingivae and arterial walls. To the best of our knowledge, this mouse model represents the first example of creating a more sustained local infection in the gingival tissues of wild-type mice and may prove to be useful for the investigation of the more natural and complete pathogenesis of the bacteria in the development of local oral and systemic diseases, such as atherosclerosis. It may also be useful for the determination of a treatment/prevention/efficacy model associated with *Pg*-induced colonization periodontitis in mice.

Correspondence to: Dr No-Hee Park, The Shapiro Family Laboratory of Viral Oncology and Aging Research, UCLA School of Dentistry, 10833 Le Conte Avenue, Los Angeles, CA 90095, USA
E-mail: nhpark@g.ucla.edu

Dr Peter L. Nara, Keystone Bio Incorporated, Suite 200, 4220 Duncan Avenue, St. Louis, MO 63110, USA
E-mail: nara@keystonebio.com

[*]Contributed equally

Key words: Porphyromonas gingivalis, intrapocket infection, periodontitis, gingipains, systemic inflammation

Introduction

Porphyromonas gingivalis (Pg) is an anaerobic Gram-negative asaccharolytic bacteria that is well-characterized among the 'red-complex' perio-pathogens known to play a critical role in the development of periodontitis (1) and systemic inflammatory diseases. *Pg* produces several known bacterial toxins, such as lipopolysaccharide (LPS), gingipains and fimbriae by local secretion, as well as incorporation into and the release of complex outer-membrane vesicles (OMVs) (2,3). Over time, these factors are destructive to the local periodontium, ultimately leading to additional dysbiotic changes, including periodontitis and the loss of clinical epithelial attachment, alveolar bone and pro-inflammatory mediators.

Among these, *Pg* LPS is known to cause inflammation by triggering innate immune responses via a unique Toll-like receptor interaction (4,5). Indeed, the authors have previously

demonstrated that the local oral delivery of *Pg* LPS induced periodontitis and alveolar bone loss in *ApoE*-deficient mice with increased amounts of pro-inflammatory cytokines both locally and systemically (6).

On the other hand, *Pg* gingipains are cysteine endo-proteases that exert their virulent effects by degrading the extracellular matrix (7-9), cleaving numerous anti-bacterial proteins in saliva and inducing systemic inflammation via the interleukin (IL)-1β/NLR family pyrin domain containing 3 inflammasome pathway (10). *Pg* produces three different types of gingipains: Arginine-gingipain A (RgpA), arginine-gingipain B (RgpB) and lysine-gingipain (Kgp) (7). Together, these gingipains not only degrade and cause epithelial cell detachment in the gingival tissues, but also degrade other proteins such as complement system, cytokines and collagen (11). Gingipains, as already mentioned, are known to be secreted, and transported to the extracellular bacterial environment in soluble and OMV-associated forms (12,13). They are also essential for the survival and pathogenicity of *Pg*, playing critical roles in the bacterial colonization, inactivation of host defenses and tissue destruction (13,14).

To date, a number of studies have developed and utilized murine models in attempts to examine the effects of *Pg* on both local and systemic alterations in various tissues (15,16). Among these, the inoculation of live bacteria into the oral cavity is frequently used (17). This model requires the application of repeated, large concentrations/volumes of live bacteria into the oral cavity (3-4 times per week over a long period of time, such as 8-12 weeks) without causing efficient pathologic outcomes, such as alveolar bone loss, the key outcome measurement of periodontitis (18,19). The injection of LPS into the gingival tissues has also been used (20,21); however, it does not account for the effects of other bacterial pathogens. Experimental periodontitis has also been induced with the placement of *Pg*-adhered ligatures into the gingival sulcus in mice (22,23). However, a concern associated with this model is that the effect of bacteria may be masked by the mechanistic trauma from the ligature. Collectively, these models do not faithfully mimic the true clinical settings in which *Pg* colonizes around the tooth to assert local and systemic effects.

The main aim of the present study was to establish a mouse model in which a small volume of *Pg* is topically applied directly into the gingival pocket to allow bacterial colonization and asserts both local and systemic effects. The wild-type mouse model developed herein demonstrated the establishment of a chronic active infection of *Pg* into the oral cavity/gingival pockets similar to that observed in a human infection/colonization with *Pg*. Topical *Pg* application into the gingival pocket resulted in local chronic colonization, as well as local and systemic inflammation, alveolar bone loss, and the accumulation of *Pg* LPS and gingipain aggregates in gingival tissue and aortic walls in mice.

Materials and methods

Animals and animal welfare considerations. A total of 50 4-week-old mice (C57BL6 background) were purchased from Jackson Laboratory. All mice were housed in a pathogen-free animal experimental facility at the University of California, Los Angeles University, under a 12-h light/dark cycle. All mice were fed normal chow and had free access to drinking water and food. The health and behavior of the mice were monitored three times a week throughout the whole duration of the experiment (12 weeks). Isoflurane (2%) and a mixture of ketamine (100 mg/kg) and xylazine (5 mg/kg) were used as anesthetics during ligature placement and phosphate-buffered saline (PBS) or bacteria inoculation. Carprofen (3 mg/kg), a pain relief drug, was also used after ligature placement to minimize the pain of the mice. The ketamine/xylazine mixture and carprofen were administered via intraperitoneal (i.p.) injection, and isoflurane was administered via inhalation. All mice were administered ketamine/xylazine prior to euthanasia to minimize suffering. Euthanasia was performed via cardiac perfusion, and the heartbeat of the mice was assessed for 5 min to verify death. All mice were euthanized as designed, apart from 1 mouse that died during the bacteria inoculation via isoflurane inhalation. All procedures were performed in compliance with the institution's policy and applicable provisions of the United States Department of Agriculture (USDA) Animal Welfare Act Regulations and the Public Health Service (PHS) Policy. The experimental protocols were approved by the Animal Research Committee (ARC) of the University of California, Los Angeles (UCLA) under ARC# 2019-057.

Creation of gingival pocket to retain topically applied PBS or bacteria in the pocket. To create a gingival pocket that allows for retaining topically applied PBS or *Pg* W83 (*Pg*) (obtained from Dr Gena D. Tribble, University of Texas School of Dentistry, Houston, TX, USA) directly into the gingival pocket, a 6-0 silk ligature was placed around the second molars for 1 week under general anesthesia using ketamine/xylazine (100 and 5 mg/kg, respectively) as previously described (6,24). After the ligature placement, all mice were administered 2 mg ampicillin and 2 mg neomycin daily by gavage for 4 days out of the 7 days in total of the ligature to facilitate the subsequent *Pg* application into the pocket and to enhance *Pg* bacterial colonization in the pocket. Following the removal of the ligature 1 week after placement, the mice were divided into 4 groups as follows: Group 1 (n=10), PBS application for 5 weeks and sacrifice at the 4th week after the final inoculation; group 2 (n=15), *Pg* application for 5 weeks and sacrifice at the 4th week after the final administration; group 3 (n=10), PBS application for 5 weeks and sacrifice at the 8th week after the final administration; and group 4 (n=15), *Pg* application for 5 weeks and sacrifice at the 8th week after the final application.

Culture of Pg and topical application of PBS or Pg directly into the gingival pocket. *Pg* was cultured based on the recommended protocol with some modifications (25). Briefly, the *Pg* culture was grown for 3-5 days on a tryptic soy blood agar plate (TSB containing 1.5% agar and 5% defibrinated sheep blood, Hemostat Laboratories) supplemented with 5 μg/ml of hemin, 0.5 μg/ml vitamin K_1 (Difco; BD Biosciences) and 0.05% L-cysteine (Sigma-Aldrich; Merck KGaA) in an anaerobic chamber at 37˚C until OD_{600} of ~1.5 [~$7.3x10^9$ colony forming U/ml (CFU/ml)]. The *Pg* culture was concentrated by centrifugation at 10,000 x g at 20˚C for 15 min and washed once with PBS before the bacterial pellet was suspended in sterile 1% methyl cellulose solution to yield a

final concentration of $5x10^{11}$ CFU/ml. The fresh *Pg* culture preparations were conducted three times a week for 5 consecutive weeks. *Pg* (10 μl) in methyl cellulose solution ($5x10^9$ CFU per gingival pocket) or 10 μl PBS prepared in methyl cellulose solution were topically applied directly onto the lingual side of the maxillary second molar into the subgingival area using the microvolume micropipette (0.1-10 μl) under the BM-LED microscope (Meiji Techno) (Fig. S1).

Sample and tissue collection. Whole blood was collected from mice by cardiac puncture under general anesthesia with isoflurane (Abbott Pharmaceutical Co. Ltd.). Following blood collection, swab samples were obtained from the gingival pocket and gingival tissue using sterile endodontic absorbent paper points (Dentsply) for semi-quantitative PCR analysis to determine the presence of *Pg* (*Pg* colonies) in the pocket. The mice were then perfused and fixed with 4% paraformaldehyde in PBS via the left ventricle for 5 min. Following perfusion, the heart and a short section of the aorta root were removed for cryosection. The maxillae of the mice were then excised and fixed with 4% paraformaldehyde in PBS, pH 7.4, at 4˚C overnight and stored in 70% ethanol solution for micro-computed tomography (μCT) analysis.

Frozen sectioning and staining of aortic root. The heart samples were embedded in cyromolds with Tissue-Tek O.C.T. compound (Sakura Finetek), and stayed frozen at -80˚C until cryo-sectioning. Frozen heart blocks were sectioned at a thickness of 20 μm at -20˚C using a CM3050 S cryostat (Leica Microsystems, Inc.) and a Cyrostar NX70 cyrostat (Thermo Fisher Scientific, Inc.) for hematoxylin and eosin (H&E; Sigma-Aldrich; Merck KGaA) and Oil Red O (Sigma-Aldrich; Merck KGaA) staining of the aortic root region for 15 min at room temperature.

Detection of Pg colonies from the gingival pocket. Swab samples taken from the gingival pocket were stored in 200 μl PBS. Genomic DNA was extracted using the Qiagen QIAamp DNA Micro kit (Qiagen, Inc.) from the sample following proteinase K (Thermo Fisher Scientific, Inc.) treatment. The protein-free purified DNA was then dissolved in 20 μl distilled water. An aliquot (5 μl) of the dissolved DNA was diluted 10-fold (to yield 50 μl diluted DNA samples). The diluted DNA sample was boiled for 5 min. The resulting lysate (4 μl) was then used directly as a template in a PCR reaction: The amount of DNA used for the PCR analysis was 1/50 of original samples taken from each swab. All PCR reactions were performed as previously described (26) using the following primers, which detect *Pg* W83-specific 16S rDNA: Forward, 5'-AGGCAGCTTGCCATACTGCG-3'; and reverse, 5'-ACTGTTAGCAACTACCGATGT-3'. Each PCR reaction was composed of a denaturation cycle of 95˚C for 8 min, followed by 50 cycles composed of one step of 95˚C for 30 sec, an annealing step of 56˚C for 30 sec, and an extension step at 72˚C for 40 sec. PCR was performed using a thermal cycler (SimpliAmp, Applied Biosystems; Thermo Fisher Scientific, Inc.). Amplified products were detected by electrophoresis. Each gel run was performed at 1% ethidium bromide on a 1% agarose gel at 110 V for 20 min. The DNA ladder was 1 Kb plus DNA ladder from Thermo Fisher Scientific, Inc. Purified *Pg* DNA (1,000 CFU) for PCR was included as a positive control to quantify the CFU of *Pg* from each pocket swab, and PCR without template DNA served as a negative control. The density of the amplified DNA was analyzed using ImageJ software Version 1.52 (National Institute of Health).

μCT and histological analysis of maxillae. The fixed maxillae were subjected to μCT scanning (Skyscan1275, Bruker-microCT Systems) using a voxel size of 20 μm^3 and a 0.5 mm aluminum filter. Two-dimensional slices from each maxilla were combined using NRecon and CTAn/CTVol programs (Bruker-microCT Systems) to form a three-dimensional reconstruction. The level of bone resorption was calculated as the distance from the palatal and mesiobuccal cement-enamel junction (CEJ) to the alveolar bone crest (ABC) of the second molars by an investigator (YB). The reading was confirmed in a blinded-manner by another individual (SK).

Following μCT scanning, the maxillae were decalcified with 5% EDTA (Sigma-Aldrich; Merck KGaA) and 4% sucrose (Sigma-Aldrich; Merck KGaA) in PBS (pH 7.4) for 3 weeks at 4˚C. The decalcification solution was changed daily. Decalcified maxillae were processed for paraffin embedding the blocks at the UCLA Translational Procurement Core Laboratory (TPCL). Blocks were sectioned at 5-μm using a microtome (Thermo Fisher Scientific, Inc.). After dewaxing with xylene, the sections were stained with hematoxylin and eosin (H&E, Sigma-Aldrich; Merck KGaA) at room temperature for 30 sec. Digital images of the stained sections were obtained using the DP72 microscope (Olympus Corporation). The clinical attachment loss (CAL) was obtained under the microscope by measuring the CEJ to the base of the pocket depth by an investigator (SK). The reading was confirmed in a blinded-manner by another individual (YB).

Antibody production for Pg lysine gingipain (Kgp) and arginine gingipain B (RgpB). As anti-*Pg* (strain W83) gingipain antibodies were of limited availability, antibodies against *Pg* gingipains were generated. Briefly, two sets of primers were designed to amplify the sequence encoding Kgp amino acids A22 to I400 and RgpB N401 to K736 from *Pg* W83 (Table SI). The amplified DNA fragments were cloned into pMCSG7 using a ligation-independent cloning (LIC) method as previously described (27), and the gingipain coding sequences were confirmed by DNA sequencing. Generated gingipain-expressing plasmids were introduced into *E. coli* BL21 (DE3) (Thermo Fisher Scientific, Inc.). Both cultures of 500 ml Luria-Bertani (LB) broth in the presence of 100 μM ampicillin were induced by the addition of 0.5 mM Isopropyl ß-D-1-thiogalactopyranoside (IPTG) at OD_{600} of 0.7-0.8 at 18˚C overnight. The induced cell cultures were pelleted by centrifugation at 6,500 x g for 10 min at 4˚C and washed with 50 mM Tris·Cl and 150 mM NaCl, pH 7.5 prior to suspension in sample buffer containing 1 mM PMSF, 20 mM β-mercaptoethanol and 20 mM imidazole. The cell suspensions were subjected to French Press (Glen Mills) to lyse the cells. The lysates were centrifuged at 6,500 x g for 20 min at 4˚C to separate the unlysed cells or insoluble proteins from the soluble proteins. Recombinant proteins were purified using Ni-NTA agarose affinity chromatography and purified proteins were analyzed by 0.1% Coomassie blue R250

(Fisher Bioreagents) in 50% methanol and 10% acetic acid solution to confirm the successful purification. The purified proteins, Kgp (7 mg/ml) and RgpB (3.8 mg/ml), were shipped to Cocalico Biologicals, Inc. for raising custom polyclonal antibody in rabbits. The produced antiserums were used for the detection of gingipains (or antibody against gingipains) in gingival tissue, blood and arterial walls.

Determination of pro-inflammatory cytokines in mouse serum. The levels of pro-inflammatory cytokines were detected as follows: Briefly, whole mouse blood was collected at 4 or 8 weeks after the final PBS or *Pg* inoculation with cardiac puncture. The serum was separated from the blood for the detection of pro-inflammatory cytokines using the Quantibody Mouse Cytokine Array kit (RayBiotech, Inc.) which allows for the determination of low levels (<20-30 pg/ml) of cytokines [e.g., granulocyte-macrophage colony-stimulating factor (GM-CSF), interferon (IFN)-γ, IL-1α, IL-1β, IL-6, IL-17, tumor necrosis factor (TNF)-α, vascular endothelial growth factor (VEGF), macrophage colony-stimulating factor (M-CSF), keratinocyte chemoattractant (KC)] from the serum samples.

Reverse transcription-quantitative PCR (RT-qPCR) for determining the expression levels of pro-inflammatory cytokines from gingival and aortic tissue. Total RNA was extracted from mouse gingival and aortic tissue using the RNeasy micro kit (Qiagen GmbH) and reverse transcribed for 5 min at 65˚C, 2 min at 25˚C and for 50 min at 45˚C cycles using the SuperScript® III Reverse Transcriptase Synthesis kit (Thermo Fisher Scientific, Inc.). Subsequently, qPCR was performed using PowerUp™ SYBR-Green Master Mix (Thermo Fisher Scientific, Inc.) or TaqMan primers (Applied Biosystems; Thermo Fisher Scientific, Inc.) for 2 min at 95˚C (one step denaturation) and amplification of DNA with 15 sec at 95˚C and 1 min at 60˚for 40 cycles as suggested by the manufacturer (Thermo Fisher Scientific, Inc.). The sequences of the primers used for RT-qPCR are presented in Table SI. Glyceraldehyde 3-phosphate dehydrogenase (GAPDH) served as a control and the fold induction was calculated using the comparative ΔCq method and are presented as relative transcript levels ($2^{-\Delta\Delta Cq}$) (28).

Detection of anti-Pg gingipains (Kgp and RgpB) and anti-Pg LPS antibodies from mouse serum. ELISA was performed on collected mouse sera to determine *Pg* Kgp-, RgpB- and LPS-specific antibodies. ELISA plates (Corning, Inc.) were coated with 100 ng Kgp or RgpB in carbonate-bicarbonate buffer (pH 9.6). ELISA plate kit pre-coated with 100 ng of *Pg* LPS were obtained from Chondrex, Inc. for the detection of anti-LPS antibody from serum (cat. no. 6222; Chondrex, Inc.). The coated wells of each plate were blocked with 2% bovine serum albumin (BSA) (Chondrex, Inc.), and various dilutions of mouse sera (1:100, 1:200, 1:400, 1:800, 1:1,600 and 1:3,200) were added to the wells and incubated for 2 h at room temperature. Anti-mouse horse radish peroxidase (HRP)-conjugated IgG antibody (cat. no. 7076, Cell Signaling Technology, Inc.) was then added at a 1:500 ratio for 1 h, followed by TMB substrate solution (eBioscience; Thermo Fisher Scientific, Inc.), and after 6 min, the resultant color intensity was recorded at 450 nm. Antibody levels as the absorbance OD value was measured using the Infinite M1000 microplate reader (Tencan).

Detection of Pg gingipain (Kgp and RgpB) and LPS aggregates in the gingiva and arterial wall of mice. For immunofluorescence analysis, formalin-fixed paraffin-embedded sections of gingival tissues and frozen sections of hearts were incubated with primary antibodies against *Pg* Kgp (rabbit polyclonal antibody), *Pg* RgpB (rabbit polyclonal antibody) and *Pg* LPS (mouse monoclonal antibody from Millipore Sigma, followed by fluorometric detection with Alexa Fluor 488-conjugated secondary antibodies (Thermo Fisher Scientific, Inc.). Sequentially, the sections were mounted on slides with VECTASHIELD® anti-fade mounting medium with 4',6-diamidino-2-phenylindole dihydrochloride (DAPI; Vector Laboratories, Inc.). The slides were then examined under a Fluoview FV200i confocal fluorescent microscope (Olympus Corporation). Digital images of the stained sections were obtained using a microscope (DP72; Olympus Corporation).

Statistical analysis. All graphs were created and statistical analyses were performed using GraphPad Prism 9.3.1 (GraphPad Software, Inc.). An unpaired Student's t-test was used for two-group comparisons, and for multiple comparisons, one-way ANOVA with Turkey's post hoc test was used. A P-value <0.05 was considered to indicate a statistically significant difference. All results from *in vitro* experiments were confirmed by at least three independent experiments. Error bars represent the mean ± SEM.

Results

Topical Pg application into the gingival pocket induces Pg colony formation in the majority of gingival pockets in mice. To retain PBS and *Pg* in the gingival pockets following the topical application, artificial pockets were created around the maxillary second molars of mice by placing silk ligature around the molars. At 1 week after the placement, the ligatures were removed and PBS or freshly cultured *Pg* were topically applied into the gingival pocket three times per week for 5 weeks. After completing the course of PBS or *Pg* application, the mice were left for 4 or 8 weeks in cages, after which they were sacrificed (Fig. 1A). As shown in Fig. 1, the swab samples from the mice receiving the topical application of PBS directly into the gingival pocket did not exhibit any presence of amplified bacterial DNA. However, the swab samples from the mice receiving the topical application of *Pg* exhibited amplified bacterial DNA bands in 4 samples (out of 9) and 7 samples (out of 10) when analyzed at 4 or 8 weeks, respectively after the final *Pg* inoculation (Fig. 1B and C). The amount of detected *Pg*/swab/mouse was ~150,000-210,000 CFU at 4 weeks and ~15,000-55,000 CFU at 8 weeks after the final *Pg* inoculation. These data indicate that the repeated topical application of *Pg* into the gingival pocket can induce and establish bacterial colony formation in the mouse gingival pocket.

Topical Pg application induces the loss of the clinical epithelial attachment and alveolar bone. The histological examination revealed that the clinical epithelial attachment loss measured from the CEJ to the base of the gingival pocket was significantly

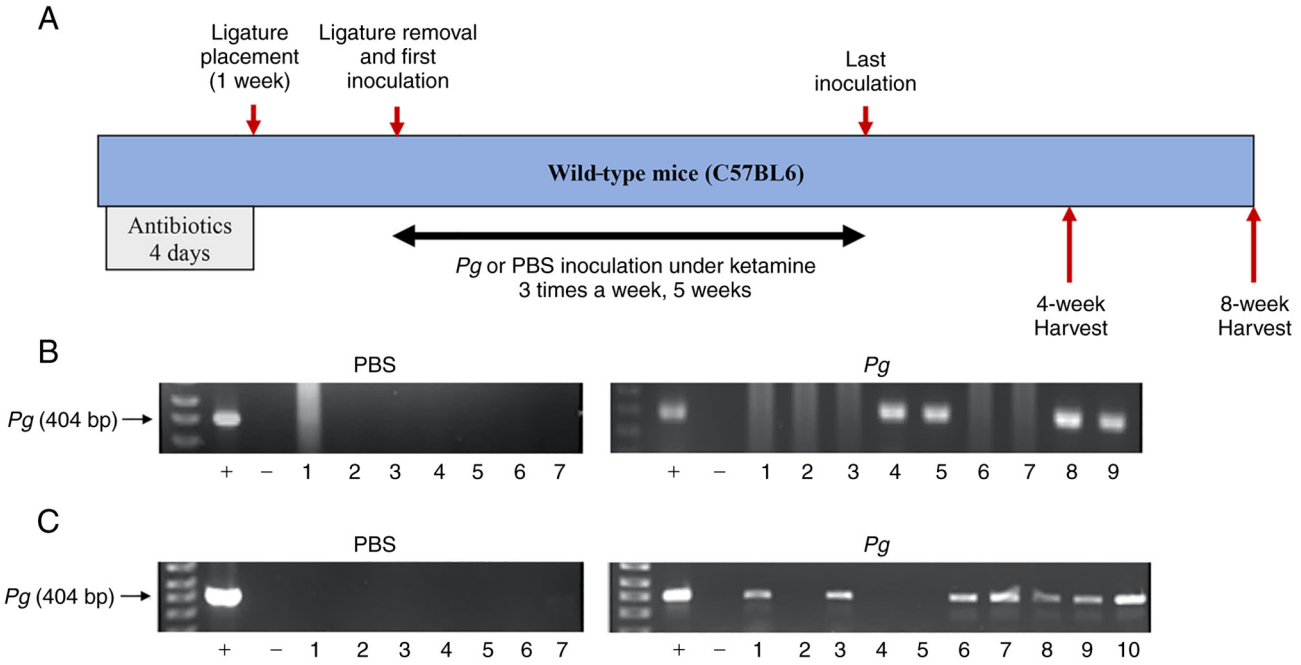

Figure 1. Research design and electrophoretic images of amplified *Pg* DNA from the gingival pocket swabs of mice collected at 4 and 8 weeks after the final PBS or *Pg* inoculation for 5 weeks. (A) Schematic diagram of the research design. (B) Electrophoretic image of amplified *Pg* DNA from mice sacrificed 4 weeks after completing the last inoculation (inoculation duration, 5 weeks). (C) Electrophoretic image of amplified *Pg* DNA from mice sacrificed 8 weeks after completing the last inoculation (inoculation duration, 5 weeks). The lanes indicate the following: +, positive control (1,000 CFU of purified *Pg* DNA); -, negative control; 1-10, samples taken from the gingival pocket. *Pg*, *Porphyromonas gingivalis*.

increased in the *Pg*-inoculated site, and the clinical attachment loss was more significant in mice at 8 weeks when compared to that in mice at 4 weeks (Fig. 2A and B), suggesting ongoing active inflammation after 4 weeks of the epithelial junction. The μCT analysis also revealed similar patterns in bone loss (Fig. 2C). When alveolar bone loss was measured from the CEJ to the crest of the alveolar bone, only the site at which *Pg* was applied (second molars) exhibited bone loss, while the sites at which *Pg* was not applied were unaltered (Fig. 2D-F), indicating the specificity of *Pg*-induced bone loss.

Topical Pg application increases the expression of pro-inflammatory cytokines in the gingival tissue. To further examine the inflammatory status around the *Pg*-inoculated soft tissue, gingival tissues around the second molars were isolated and subjected to RT-qPCR analysis for determining the expression levels of IL-1β, IL-6, TNF-α, inducible nitric oxide synthase (iNOS) and IL-17. The expression levels of pro-inflammatory cytokines, including IL-1β and IL-6 were upregulated by the 4th and 8th week when compared with the controls with PBS treatment (Fig. 3A and B). The other screened cytokines, such as TNF-α, iNOS and IL-17 were also upregulated, although the increases were not statistically significant (Fig. 3C-E). These data indicated that the topical *Pg* application into the gingival pocket induced local inflammation around the tooth.

Topical Pg application directly into the gingival pocket induces systemic inflammation. As periodontitis embodies systemic inflammation, the levels of inflammatory cytokines in serum were examined to determine whether the topical *Pg* application can induce systemic inflammation. In mice receiving the topical *Pg* application, significantly higher levels of pro-inflammatory cytokines, such as TNF-α, IL-13, IL-1β, IL-17, KC and IFN-γ, were detected in serum compared to those in mice receiving PBS when measured at the 4th week after the final *Pg* or PBS inoculation (Fig. 4). However, higher levels of IL-1β and KC were detected only in the serum of mice receiving *Pg* compared to those receiving PBS when measured at the 8th week after the final *Pg* or PBS inoculation (Fig. 4). The serum levels of IL-1α , IL-2, IL-3, IL-4, IL-5, IL-6, IL-9, IL-10, IL-12, M-CSF, GM-CSF, VEGF, monocyte chemotactic protein-1 (MCP-1) or regulated upon activation, normal T cell expressed and secreted (RANTES) were not markedly altered by the *Pg* inoculation regardless of the time point (4th or 8th week) after the final *Pg* inoculation (Fig. S2).

Anti-Pg gingipain and anti-Pg LPS antibodies detected in the sera of mice receiving the topical Pg application into the gingival pocket. Anti-*Pg* gingipain and *Pg* LPS antibodies in the blood were measured using *Pg* gingipain (Kgp and RgpB) and *Pg* LPS as probes using an ELISA-based assay. Both anti-gingipain and anti-LPS antibodies were detected in sera of mice receiving the topical *Pg* application; however, no such antibodies (or basal level) were detected in mice receiving the topical PBS application (Fig. 5).

Pg gingipain and LPS are identified in the gingival tissues of mice receiving the topical application of Pg into the gingival pocket. Gingipains and LPS are crucial virulent factors released in both soluble mediators and in OMVs by *Pg*, and they are frequently found in tissues (2,3). In the present study, to detect whether these proteins are present in the gingival tissue of mice receiving the topical *Pg* application, recombinant proteins for gingipain (Kgp and RgpB) were generated and used to raise

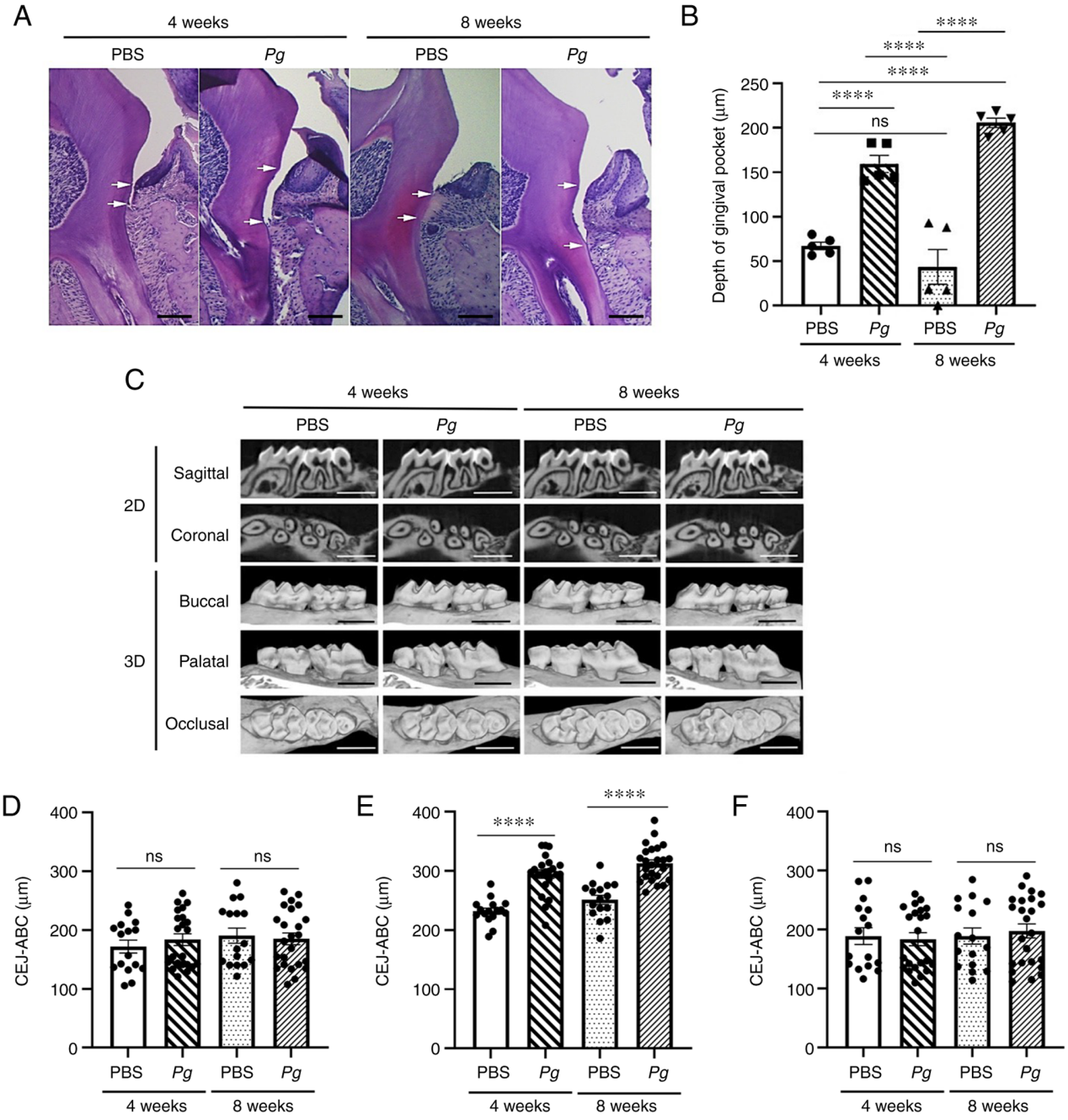

Figure 2. Topical *Pg* application directly into the gingival pocket induces clinical epithelial attachment loss and alveolar bone loss. (A) Representative images of hematoxylin and eosin staining of the maxillary second molar and periodontal tissue. Scale bar, 100 μm. White arrows indicate the CEJ. (B) Depth of gingival pocket histologically measured at the mesiobuccal pocket of the maxillary second molars from CEJ to the base of pocket. ****P<0.001 (n=5). Results represent the mean ± SEM. (C) Representative two or three dimensional μCT images of mice maxillae. The mice were sacrificed at 4 (right) or 8 (left) weeks after the final PBS or *Pg* inoculation. Scale bar, 1 mm. The average distance from the palatal and mesiobuccal CEJ to the ABC of (D) upper first molar, (E) second molar, and (F) third molar. Results represent the means ± SEM performed in ten samples. ****P<0.001. ns, not significant (P>0.05); *Pg, Porphyromonas gingivalis*; CEJ, cement-enamel junction; ABC, alveolar bone crest.

antibodies against them (Fig. S3). For LPS, the commercially available antibody was used. Immunofluorescence staining using these antibodies revealed that both gingipain and LPS were detected at the site at which *Pg* was inoculated (Fig. 6). These data indicate that local *Pg* LPS and gingipains may, in part, be responsible for the gingival inflammation.

Pg gingipain and Pg LPS are found in the aortic roots of mice receiving the topical Pg application directly into the gingival pocket. The authors have previously reported that ligature-induced periodontitis causes the exacerbation of atherosclerotic lesions in *ApoE*-deficient mice (6,24). In the present study, to evaluate the status of the atherosclerosis in these wild-type mice, the hearts and the aortic roots were harvested together. No changes were observed in the histological features of lipid deposition that are indicative of atherosclerosis (Fig. S4). Subsequently, the aortic roots were further examined for evidence of *Pg* gingipains and *Pg* LPS aggregates. Immunofluorescence staining revealed distinct focal signals of both *Pg* gingipains and *Pg* LPS in the aortic

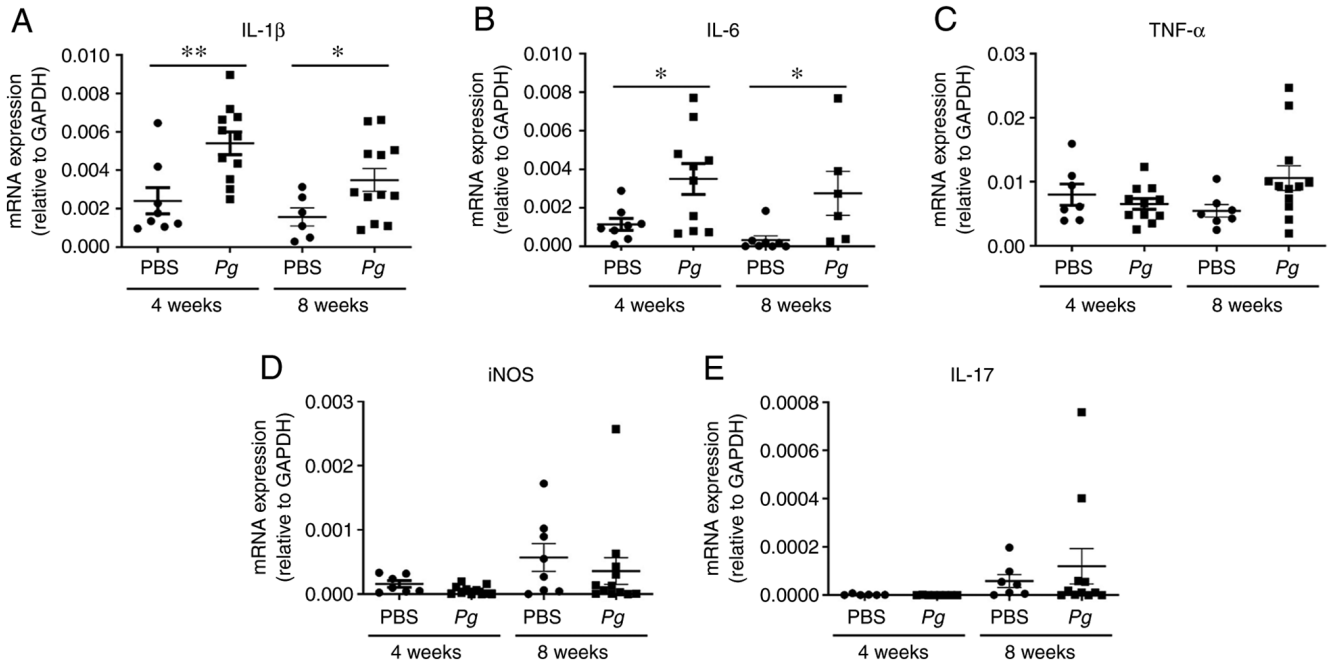

Figure 3. Topical *Pg* application directly into the gingival pocket increases the expression of pro-inflammatory cytokines in gingival tissues. Reverse transcription-quantitative PCR of pro-inflammatory cytokines (A) IL-1β, (B) IL-6, (C) TNF-α, (D) iNOS, and (E) IL-17 from the gingival tissue of second molars of mice receiving ligature placement for 1 week followed by PBS or *Pg* inoculation into the gingival pocket. The cytokine levels were determined from the tissues obtained at 4 or 8 weeks after the final *Pg* inoculation. GAPDH served as the loading control. *P<0.05 and **P<0.01. Results represent the mean ± SEM performed in triplicate; n=8-12 mice per group. Each dot represents a result from 1 mouse. *Pg, Porphyromonas gingivalis*; IL, interleukin; TNF-α, tumor necrosis factor α; iNOS, inducible nitric oxide synthase.

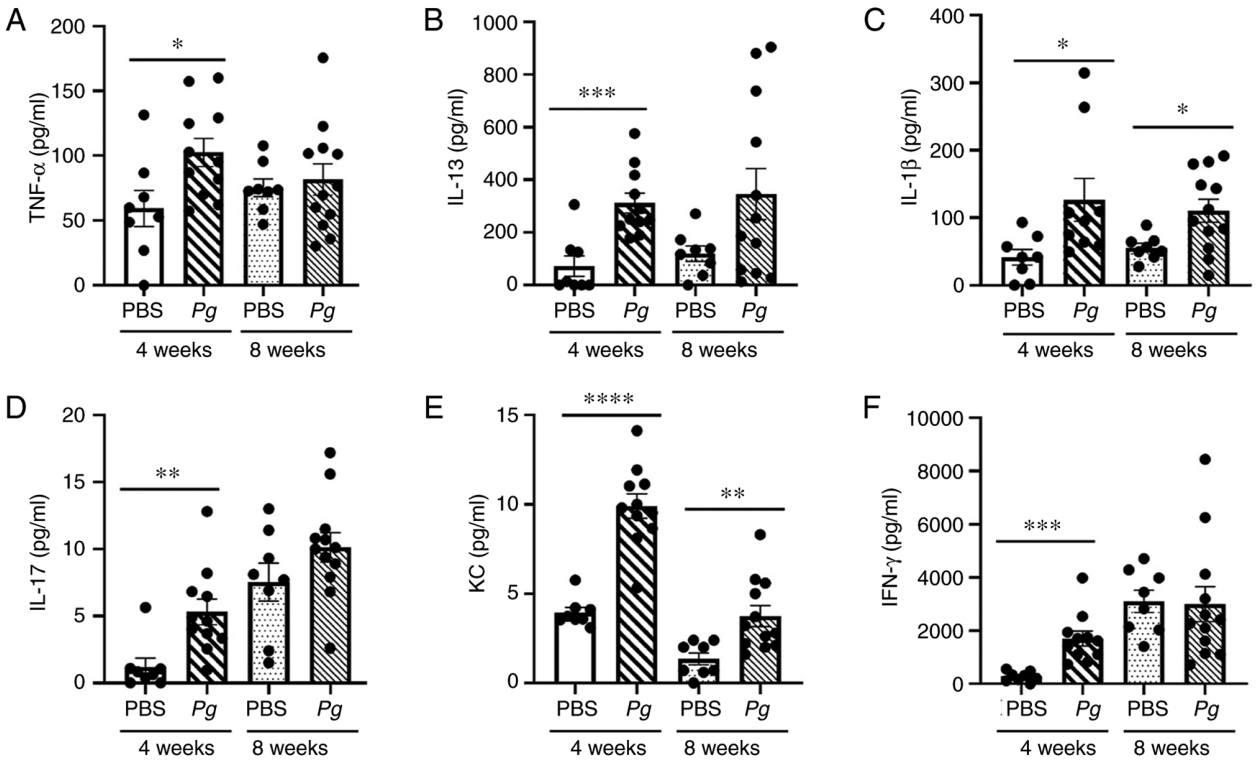

Figure 4. Topical *Pg* application directly into the gingival pocket induces systemic inflammation. ELISA measuring the levels (pg/ml) of (A) TNF-α, (B) IL-13, (C) IL-1β, (D) IL-17, (E) KC, and (F) IFN-γ from mouse sera at 4 and 8 weeks after the final PBS or *Pg* inoculation. *P<0.05, **P<0.01, ***P<0.005 and ****P<0.001 determined using one-way ANOVA. Results represent the mean ± SEM; n=8-12 mice per group. Each dot represents a result from 1 mouse. *Pg, Porphyromonas gingivalis*; IL, interleukin; TNF-α, tumor necrosis factor α; KC, keratinocyte chemoattractant; IFN-γ, interferon γ.

walls of mice receiving the topical *Pg* application (Fig. 7; the second and fourth rows in each panel). By contrast, there were no signals in the aortic roots of mice receiving the topical PBS application (Fig. 7; the first and third rows in each panel).

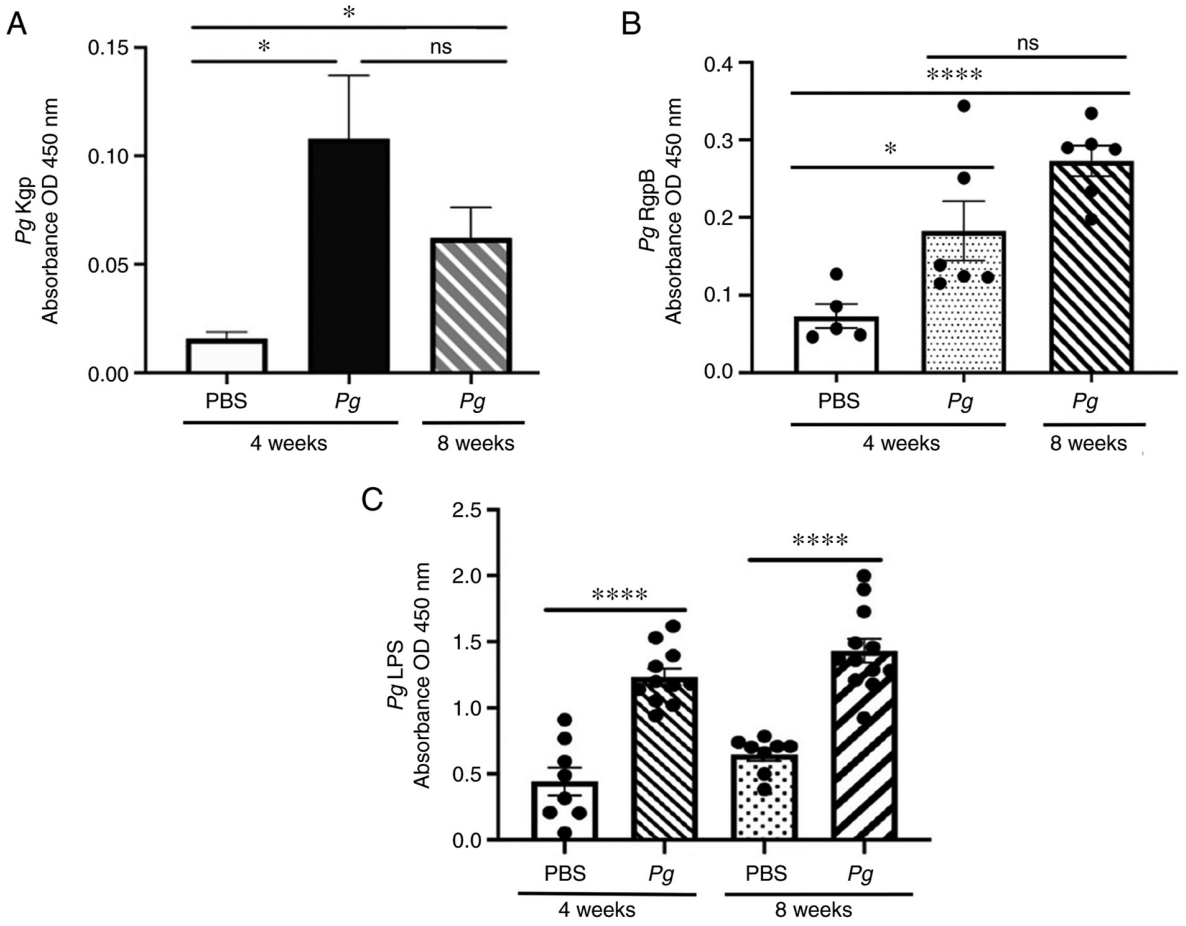

Figure 5. Anti-*Pg* gingipain and anti-*Pg* LPS antibodies are detected in the sera of mice receiving *Pg* inoculation in the gingival pocket. (A) ELISA was used to measure the serum levels of anti-Kgp antibody. Mouse sera examined 4 weeks after the final PBS inoculation (PBS) exhibited only background levels of Kgp antibody. Significance was analyzed using an unpaired t-test. Tested sera were diluted 1:800. Error bars indicate the mean ± SEM. (B) ELISA was used to measure the serum level of anti-RgpB antibody. Mouse sera examined 4 weeks after the final PBS inoculation (PBS) exhibited only background levels of RgpB antibody. Significance was analyzed using an unpaired t-test. Tested sera were diluted 1:800. Error bars indicate the mean ± SEM. *P<0.05. (C) ELISA was used to measure the serum level of anti-*Pg* LPS antibody. Anti-*Pg*-LPS IgG levels in mouse sera were measured using a Mouse Anti-*Pg*-LPS antibody assay kit according to the manufacturer's protocol. Tested sera were diluted 1:800. Absorbance was read at 450 nm using a microplate reader. Significance was analyzed using an unpaired t-test. Error bars indicate the mean ± SEM. *P<0.05 and ****P<0.001, determined using one-way ANOVA. ns, not significant (P>0.05). Results represent the mean ± SEM. *Pg*, *Porphyromonas gingivalis*; LPS, lipopolysaccharide; Kgp, lysine-gingipain; RgpB, arginine-gingipain B.

Discussion

To date, to the best of our knowledge, no animal models have been reported that faithfully mimic the clinical settings in which perio-pathogens, including *Pg* colonize around a tooth. In the present study, a mouse model of *Pg* colonization was successfully established, in which *Pg* was topically and directly applied into an artificially created gingival pocket. This was able to induce more chronic active periodontitis and other systemic effects, in part due to the prolonged colonization of *Pg* around the tooth.

Mice are not the natural host of *Pg* (29). For this reason, several methods have been developed to mimic a human *Pg* associated periodontal disease state in mice, including the inoculation of live bacteria into the oral cavity (17). Although this method has been widely used to study and demonstrate the local and systemic effects of *Pg* (30,31), its general application to the whole oral cavity and the use of the high concentrations and exhaustive repeated applications (3-4x/week over a period of 8-12 weeks) without causing drastic alveolar bone loss, renders it difficult to examine the sole effects of bacterial colonization around the tooth to the local and systemic outcomes. The model established herein is distinct from previously reported models, in that the ligature was only used for 1 week to create gingival pocket, after which the ligature was removed and *Pg* was locally and topically applied on one tooth for 5 weeks. Within this relatively short period of time, bacterial colonization was efficiently established and conferred local effects by causing alveolar bone loss on the applied tooth only, as well as systemic effects, as demonstrated by the presence of *Pg* pathogen in the vascular system.

One of the major concerns with the conventional periodontitis model (e.g., oral inoculation) is a potential systemic effect via the gastrointestinal (GI) tract by swallowing the inoculated bacteria. In the model in the present study, although an attempt was made to apply *Pg* locally in a small volume, this potential still exists as locally administered *Pg* can be subsequently swallowed by the mouse. On the other hand, knowing this shortcoming, this mouse model was developed strategically by creating a gingival pocket with a ligature (to maximize the administration and colonization of *Pg* locally) and topically applying *Pg* for only 5 weeks (to allow the colonization of

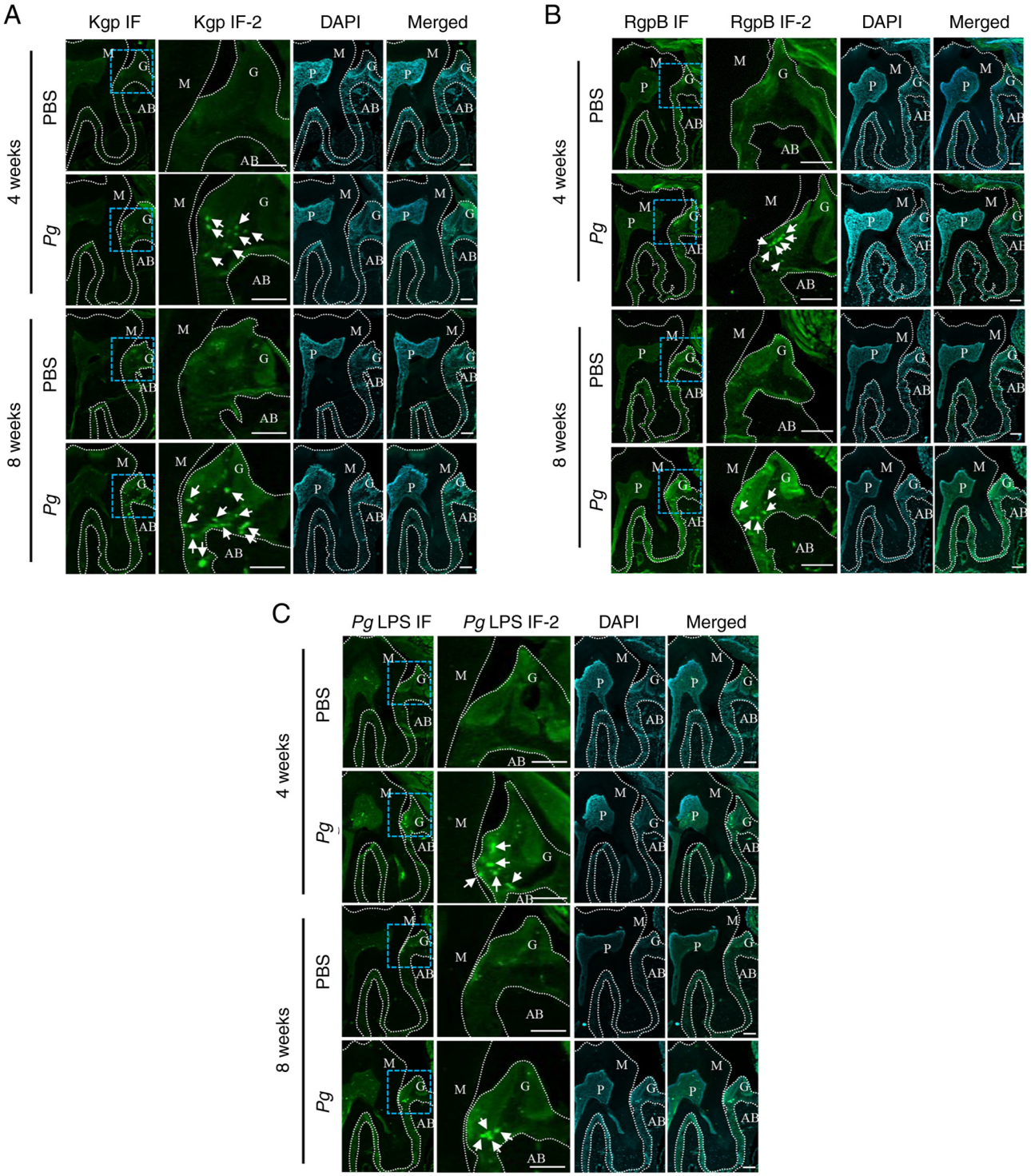

Figure 6. *Pg* gingipains and LPS aggregates are present in the gingival tissues of mice receiving the topical *Pg* inoculation into the gingival pocket. (A) IF analysis using Kgp. PBS and *Pg* were from the mice sacrificed at 4 or 8 weeks after the final PBS or *Pg* inoculation. Kgp IF-2 is the higher-magnified image of blue-dotted square in Kgp IF. Kgp (bright green color dots, arrows) was present only in the gingival tissue of mouse receiving topical *Pg* not in those receiving PBS. (B) IF analysis using RgpB. PBS and *Pg* were from the mice sacrificed at 4 or 8 weeks after the final PBS or *Pg* inoculation. RgpB IF-2 is the higher-magnified image of blue-dotted square in RgpB IF. The RgpB (bright green color dots, arrows) was present only in the gingival tissue of mouse receiving topical *Pg* not in those receiving PBS. (C) IF analysis using *Pg* LPS. PBS and *Pg* were from the mice sacrificed at 4 or 8 weeks after the final PBS or *Pg* inoculation. *Pg* LPS -2 is the higher-magnified image of blue-dotted square in *Pg* LPS IF. The *Pg* LPS (bright green color dots, arrows) was present only in the gingival tissue of mouse receiving topical *Pg* not in those receiving PBS. DAPI was heavily stained in pulpal and gingival tissues. Scale bars, 100 μm. M, upper second molar; G, gingival tissue; AB, alveolar bone; P, pulpal tissue; *Pg, Porphyromonas gingivalis*; IF, immunofluorescence; LPS, lipopolysaccharide; Kgp, lysine-gingipain; RgpB, arginine-gingipain B.

bacteria around the tooth), and leaving the mice for an additional 4 and 8 weeks without any further *Pg* application (to allow the clearance of bacteria from the GI tract and systemic circulation as a direct result of *Pg* inoculation). It was reasoned that terminating the oral inoculation of bacteria and leaving the mice for an additional 4 or 8 weeks would allow a sufficient

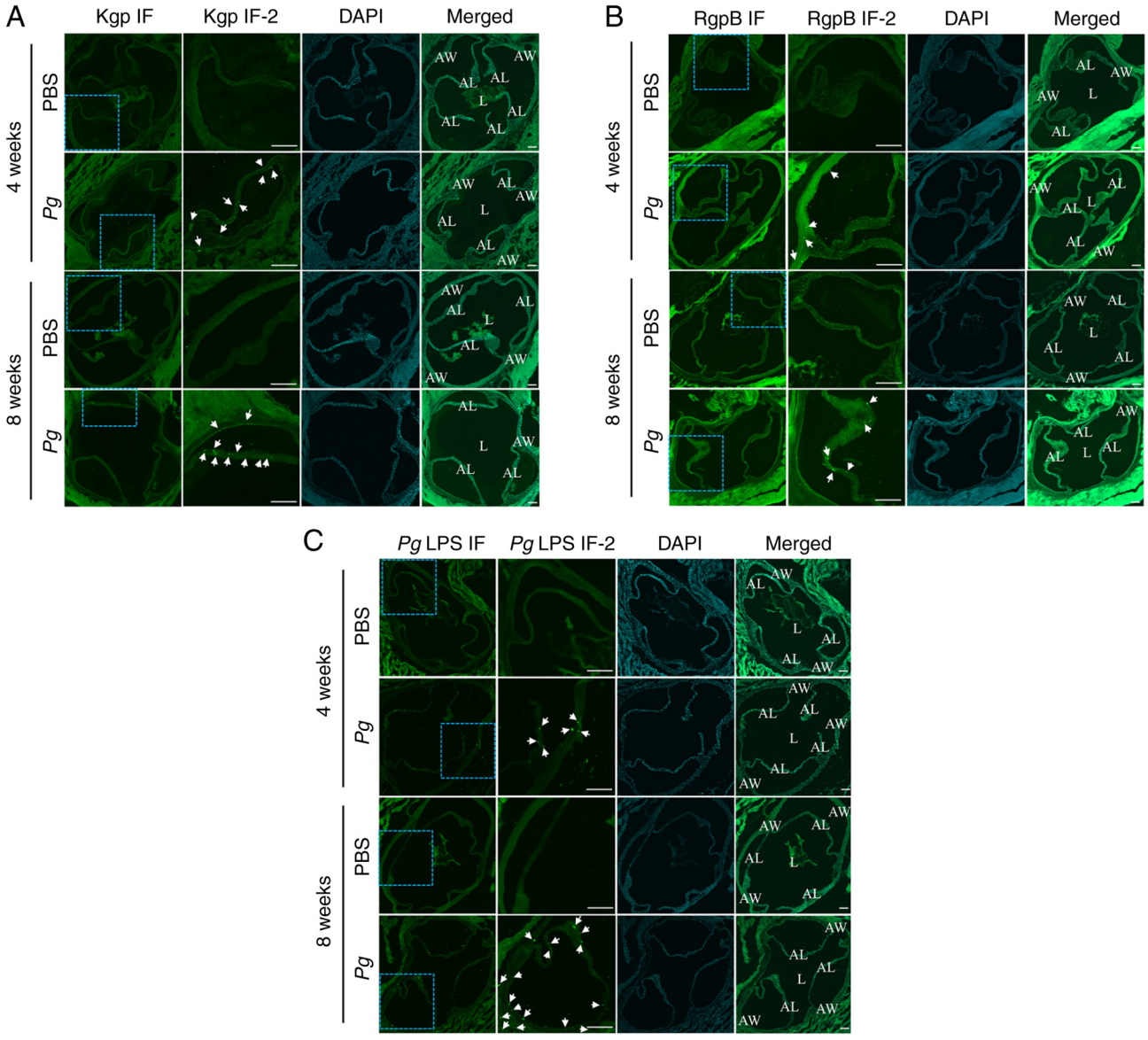

Figure 7. *Pg* gingipain and *Pg* LPS aggregates are found in the aortic roots of mice receiving *Pg* inoculation into the gingival pocket. (A) IF analysis using Kgp. PBS and *Pg* were from the mice sacrificed at 4 or 8 weeks after the final PBS or *Pg* inoculation. Kgp IF-2 is the higher-magnified image of blue-dotted square in Kgp IF. The RgpB (bright green color dots, arrows) was present only in the aortic leaflet and aortic wall of mouse receiving topical *Pg*, not in those receiving PBS. (B) IF analysis using RgpB. PBS and *Pg* were from the mice sacrificed at 4 or 8 weeks after the final PBS or *Pg* inoculation. RgpB IF-2 is the higher-magnified image of blue-dotted square in RgpB IF. The RgpB (bright green color dots, arrows) was present only in the aortic leaflet and aortic wall of mouse receiving topical *Pg*, not in those receiving PBS. (C) IF analysis using *Pg* LPS. PBS and *Pg* were from the mice sacrificed at 4 or 8 weeks after the final PBS or *Pg* inoculation. *Pg* LPS -2 is the higher-magnified image of blue-dotted square in *Pg* LPS IF. The LPS (bright green color dots, arrows) was present only in the aortic leaflet and aortic wall of mouse receiving topical *Pg*, not in those receiving PBS. Nuclei of cells were localized with DAPI staining. Scale bars, 100 μm. L, lumen; AW, aortic wall; AL, aortic leaflet; *Pg, Porphyromonas gingivalis*; IF, immunofluorescence; LPS, lipopolysaccharide; Kgp, lysine-gingipain; RgpB, arginine-gingipain B.

amount of time for bacterial ingestion via the GI tract to be reduced and to maximize bacterial colonization on the tooth surface. Indeed, it has been reported that the average half-life of bacteria clearance from blood is 2-10 min in mice (32). Therefore, it is conceivable that the systemic effects that were observed in the present study may primarily be derived from the colonized *Pg* around the tooth through the gingival tissues, rather than by the accidental swallowing of the inoculated bacteria via the GI tract.

It is noteworthy that not all mice inoculated with *Pg* topically developed colonies around the second molar tooth. Indeed, the present study demonstrated that 45-70% of mice established *Pg* colonies around the second molars (Fig. 1). As this was a pilot study, it is conceivable that increasing the numbers of adjacent molar teeth would increase the number of positive animals and may reflect even better the human oral condition. The detected amount of *Pg*/swab/mouse was higher at 4 weeks (~150,000-210,000 CFU) when compared to that at 8 weeks (~15,000-55,000 CFU). The higher numbers observed at 4 weeks may be the result of carryover from the final inoculation of the bacterial colonies. Alternatively, the lower numbers observed at 8 weeks may be due to increasing host defense responses (e.g., anti-*Pg* antibodies toward *Pg* due to the chronic infection status). Collectively, these data indicate

that the establishment of *Pg* colonies even in one second molar appears to be directly linked to the ongoing more chronic colonization and resulting systemic virulent effects of *Pg* in the mice.

It is noteworthy that even though only a small number of teeth were inoculated and colonized, systemic manifestations were readily observed, suggesting a relatively potent inflammatory capacity of *Pg* for the murine host as observed herein. Moreover, given the relatively limited number of total bacteria in the oral cavity, the observance of LPS and gingipains at distant tissue sites (aortic tissues) may suggest again that these bacterial toxins are readily transported presumably via OMVs originating in the gums. Multiple studies have concluded similar findings. Recently, He *et al* (33) demonstrated in a mouse model that released OMVs from *Pg* exerted potent cytotoxic effects on lung epithelial cells; *Pg* OMVs revealed their ability to induce the apoptosis of lung epithelial cells and disrupt the epithelial barrier system. They concluded from their experimental design that these observations suggest that OMVs deliver their pathogenic factors from the oral cavity to respiratory organs without the direct translocation of *Pg* itself (33). O'Brien-Simpson *et al* (34) similarly demonstrated that *Pg*-infected cells and the RgpA-Kgp OMV complexes at low concentrations stimulated secretory intercellular adhesion molecule 1, IL-8, IL-6 and MCP secretion from cultured human epithelial (KB) and fibroblast (MRC-5) cells. However, at high concentrations, a reduction in the level of these mediators was observed (34). By contrast, macrophage inflammatory protein 1 and IL-1 were stimulated only at high *Pg* cell concentrations. *Pg*-infected cells and the RgpA-Kgp OMV complexes were shown to induce the apoptosis of KB and MRC-5 cells in a time- and concentration-dependent manner (34). These data suggest that the RgpA-Kgp complexes penetrate the gingival connective tissue; at low concentrations distal from the plaque, the complexes stimulate the secretion of pro-inflammatory mediators, while at high concentrations proximal to the plaque, they induce apoptosis and attenuate the secretion of pro-inflammatory mediators.

Previously, it was demonstrated that ligature placement in the gingival pocket enhanced expression of pro-inflammatory cytokines in both the local gingiva, aortic tissue and serum, and that *Pg*. LPS further exacerbated these expression levels in *ApoE*-deficient mice (6,24). *Pg* LPS, the major glycolipids present at the surface of the *Pg*, is one of the virulent factors in *Pg*. It has recently been demonstrated that *Pg* LPS weakly induces pro-inflammatory cytokine production in mice by activating Toll-like receptor 4 (35). Similarly, the present study found that the local inoculation of *Pg* induced the expression of pro-inflammatory cytokines even in wild-type mice (Figs. 3 and 4). This is also in line with a previous report in which both wild-type and *ApoE*-deficient mice exhibited an increased expression of pro-inflammatory cytokines in serum when challenged by *Pg* via the oral cavity (36).

Macrophages are important immune cells that are known to be associated with atherosclerosis. In particular, macrophages produce TNF-α that alters the phenotypes of vascular smooth muscle cells and contributes to the development of atherosclerosis (37). TNF-α-producing M1 macrophages are crucial producers of pro-inflammatory cytokines and are activated by stimuli, such as LPS (38). Therefore, the prolonged production of LPS from locally accumulated Pg may promote macrophages to undergo M1 polarization, affecting the local diseases (e.g., periodontitis) and the systemic diseases (e.g., atherosclerosis).

In the mouse model in the present study, *Pg* LPS and gingipains were detected in the gingival tissues (Fig. 6C) and the aortic walls (Fig. 7C). Such findings as discussed above suggest that *Pg* OMVs containing these toxins may have penetrated through the epithelial barriers and reside in the gingival tissues as well as in the blood stream. Indeed, a previous study demonstrated that *Pg* OMVs and occasionally PG DNA was found to be localized into squamous epithelium and capillary endothelium in patients with periodontitis (39). *Pg DNA* was also detected in the aortic walls (40-42). These results however, are complicated by the fact that *Pg*, similar to several other Gram-negative bacterial OMVs carry numerous forms of both functional RNA and DNA transcripts. Without controlling for a more direct means of detecting the whole bacterial cell, one cannot conclude what the source of the DNA is in these tissues. It is becoming clearer that *Pg* OMV, as well as other species OMVs, such *H. Pylori* in which a cell modulating and transforming cell factor CagA are found circulating in human serum samples of infected patients' chronic gastritis (43).

The rather limited topical application of *Pg* into the gingival pocket of the second molars appears to have led to a more chronic active colonization, possibly inducing the secretion of free bacterial toxins or in the form of OMVs containing gingipains and LPS into the blood or lymphatics. It cannot be discounted that a planktonic form of *Pg* is released from the bacterial colony in the sulcus with *Pg* penetration/transmigration through the gingival epithelial tissues and the aortic endothelial layers and/or through a 'Trojan Horse' cellular macrophage mechanism.

Pg gingipains are cysteine proteases that assert their virulent effects by degrading the extracellular matrix (7-9). It has been demonstrated that *Pg* gingipains disrupt epithelial barrier functions by degrading JAM1, a tight junction-associated protein, leading to *Pg* penetration into the tissues (44). *Pg* produces three different types of gingipains: Arginine-gingipain A (RgpA), arginine-gingipain B (RgpB) and lysine-gingipain (Kgp) (7). Herein, by generating recombinant proteins, antibodies against RgpB and Kgp were developed (Fig. S3). Using these antibodies, *Pg* gingipains were detected in the gingival tissues (Fig. 6A and B). Of note, anti-*Pg* gingipain and LPS antibodies were detected in the serum (Fig. 5A and B), while *Pg* gingipains and LPS were also found in the aortic walls (Fig. 7). Such finding suggests that the effects of *Pg* gingipains and LPS are at both local and systemic levels, asserting ECM-degrading functions and assisting in *Pg* penetrations into different parts of the body, including the aorta. Alternatively, it is possible that the OMV containing LPS can be released from the *Pg*, transmigrating from the gingival sulcus through the blood to proximal tissue organs, such as the aorta.

Wild-type mice do not develop lipid deposition at the intercostal arteries, at the junction of the aorta to the heart, unless fed a high-fat diet for prolonged period of time (45). Even with the high-fat diet in mice with an *ApoE*-deficient background, the development of atherosclerosis is attenuated

in the presence of statins (24,46-49). As such, it is highly probable that additional factors, such as high serum lipid levels are required in order to create an inflammatory environment that can drive atherosclerosis development in the aortic areas. Additionally, it is known that pro-inflammatory responses are highly locally regulated and thus may be inhibited to assure intra-cellular survival.

As demonstrated herein, while anti-*Pg* LPS and anti-*Pg* RgpB antibodies were progressively present at higher levels at 8 weeks as compared with 4 weeks, the anti-*Pg* Kgp antibody level was decreased at 8 weeks, although the difference was not statistically significant (Fig. 5). However, in a murine lesion model, O'Brien-Simpson *et al* (8) demonstrated that the virulence of Kgp was more significant when compared to that of RgpB, suggesting that the potency of these two gingipains was functionally different. RgpB and Kgp are encoded from different genes, and they are also post-translationally regulated (50-52). As such, it would of interest to further examine their regulations and functions as *Pg* colonizes around the tooth in a time-dependent manner; this may more easily studied using the model presented herein.

The accumulated *Pg* gingipain/LPS aggregates in the arterial wall are known to be associated with the development of atherosclerosis (53). It is highly probable that anti-gingipain antibodies are associated with human periodontitis and may be important for the control of periodontitis. While targeting gingipains may provide some therapeutic improvement, targeting the whole bacteria with a precision biological such as monoclonal antibody would be significantly more efficacious, as it would result in the complete cessation of all bacterial toxins from the local and systemic circulation and would possibly allow for the re-establishment of a more normal oral microbiome.

In conclusion, the present study established the development *in vivo* of a chronic *Pg* periodontal infection/colonization of a wild-type mouse model that is more bacteriologically similar to that of the human condition. The advantages of this animal model include: i) Demonstration of the proof-of-principle that topically applied *Pg* bacteria into the small artificially created gingival pocket leads to a pro-longed bacterial colonization around the tooth and induces subsequent local and systemic inflammatory responses; ii) the establishment of a mouse model that can provide a strategy with which to evaluate the local effects of specific strains of bacteria, such as *Pg*; and iii) the utilization of this mouse model to further study other systemic diseases. In particular, as elevated cholesterol levels are closely associated with the development of atherosclerosis and Alzheimer's disease (54,55), the further utilization of this novel *Pg* periodontal model applied in *ApoE*-deficient mice may prove to be useful for the further examination of the pathogenesis of these periodontitis-related toxins and systemic diseases, as well as of the therapeutic efficacy of different treatment modalities, including *Pg* monoclonal antibodies and vaccines.

Acknowledgements

The authors would like to thank Dr Marc Penn and Dr Dan Sindelar from Keystone Bio Inc for their critical reading of the manuscript and for providing constructive criticisms.

Funding

The present study was supported in part by the research funds awarded from the UCLA Chancellor's Office and Keystone Bio Inc. and the National Institute of Dental and Craniofacial Research (NIDCR)/NIH under the Award Number DE026758.

Availability of data and materials

The datasets used and/or analyzed during the current study are available from the corresponding author on reasonable request.

Authors' contributions

NHP, RK and PLN were involved in the conceptualization of the study. SK, YB, JK, BT and DK performed the experiments and participated in data analysis. CC and HTT were responsible for THE *Pg* culture and gingipain antibody production. SHL performed the RT-qPCR analyses. SK, YB, RK and NHP were involved in the discussion and interpretation of the results. SK, RK, PN, and NHP drafted the manuscript. SK, YB, JK and CC confirm the authenticity of all the raw data. All authors have read and approved the final manuscript.

Ethics approval and consent to participate

All procedures were performed in compliance with the institution's policy and applicable provisions of the United States Department of Agriculture (USDA) Animal Welfare Act Regulations and the Public Health Service (PHS) Policy. The experimental protocols were approved by the Animal Research Committee (ARC) of the University of California, Los Angeles (UCLA) under ARC# 2019-057.

Patient consent for publication

Not applicable.

Competing interests

The authors declare that they have no competing interests.

References

1. Darveau RP: Periodontitis: A polymicrobial disruption of host homeostasis. Nat Rev Microbiol 8: 481-490, 2010.
2. Hajishengallis G, Wang M and Liang S: Induction of distinct TLR2-mediated proinflammatory and proadhesive signaling pathways in response to porphyromonas gingivalis fimbriae. J Immunol 182: 6690-6696, 2009.
3. Takii R, Kadowaki T, Baba A, Tsukuba T and Yamamoto K: A functional virulence complex composed of gingipains, adhesins, and lipopolysaccharide shows high affinity to host cells and matrix proteins and escapes recognition by host immune systems. Infect Immun 73: 883-893, 2005.
4. Hiyari S, Atti E, Camargo PM, Eskin E, Lusis AJ, Tetradis S and Pirih FQ: Heritability of periodontal bone loss in mice. J Periodontal Res 50: 730-736, 2015.
5. Liu R, Desta T, Raptis M, Darveau RP and Graves DT: P. gingivalis and E. coli lipopolysaccharides exhibit different systemic but similar local induction of inflammatory markers. J Periodontol 79: 1241-1247, 2008.

6. Suh JS, Kim S, Boström KI, Wang CY, Kim RH and Park NH: Periodontitis-induced systemic inflammation exacerbates atherosclerosis partly via endothelial-mesenchymal transition in mice. Int J Oral Sci 11: 21, 2019.
7. Imamura T: The role of gingipains in the pathogenesis of periodontal disease. J Periodontol 74: 111-118, 2003.
8. O'Brien-Simpson NM, Paolini RA, Hoffmann B, Slakeski N, Dashper SG and Reynolds EC: Role of RgpA, RgpB, and Kgp proteinases in virulence of Porphyromonas gingivalis W50 in a murine lesion model. Infect Immun 69: 7527-7534, 2001.
9. Pike RN, Potempa J, McGraw W, Coetzer TH and Travis J: Characterization of the binding activities of proteinase-adhesin complexes from Porphyromonas gingivalis. J Bacteriol 178: 2876-2882, 1996.
10. Ding PH, Yang MX, Wang NN, Jin LJ, Dong Y, Cai X and Chen LL: Porphyromonas gingivalis-induced NLRP3 inflammasome activation and its downstream interleukin-1beta release depend on caspase-4. Front Microbiol 11: 1881, 2020.
11. Fitzpatrick RE, Wijeyewickrema LC and Pike RN: The gingipains: Scissors and glue of the periodontal pathogen, Porphyromonas gingivalis. Future Microbiol 4: 471-487, 2009.
12. Gui MJ, Dashper SG, Slakeski N, Chen YY and Reynolds EC: Spheres of influence: Porphyromonas gingivalis outer membrane vesicles. Mol Oral Microbiol 31: 365-378, 2016.
13. Guo Y, Nguyen KA and Potempa J: Dichotomy of gingipains action as virulence factors: From cleaving substrates with the precision of a surgeon's knife to a meat chopper-like brutal degradation of proteins. Periodontol 2000 54: 15-44, 2010.
14. Grenier D, Roy S, Chandad F, Plamondon P, Yoshioka M, Nakayama K and Mayrand D: Effect of inactivation of the Arg- and/or Lys-gingipain gene on selected virulence and physiological properties of porphyromonas gingivalis. Infect Immun 71: 4742-4748, 2003.
15. Lalla E, Lamster IB, Feit M, Huang L and Schmidt AM: A murine model of accelerated periodontal disease in diabetes. J Periodontal Res 33: 387-399, 1998.
16. Graves DT, Kang J, Andriankaja O, Wada K and Rossa C Jr: Animal models to study host-bacteria interactions involved in periodontitis. Front Oral Biol 15: 117-132, 2012.
17. Baker PJ, Evans RT and Roopenian DC: Oral infection with Porphyromonas gingivalis and induced alveolar bone loss in immunocompetent and severe combined immunodeficient mice. Arch Oral Biol 39: 1035-1040, 1994.
18. Bainbridge B, Verma RK, Eastman C, Yehia B, Rivera M, Moffatt C, Bhattacharyya I, Lamont RJ and Kesavalu L: Role of Porphyromonas gingivalis phosphoserine phosphatase enzyme SerB in inflammation, immune response, and induction of alveolar bone resorption in rats. Infect Immun 78: 4560-4569, 2010.
19. Baker PJ, Dixon M, Evans RT and Roopenian DC: Heterogeneity of Porphyromonas gingivalis strains in the induction of alveolar bone loss in mice. Oral Microbiol Immunol 15: 27-32, 2000.
20. Dumitrescu AL, Abd-El-Aleem S, Morales-Aza B and Donaldson LF: A model of periodontitis in the rat: Effect of lipopolysaccharide on bone resorption, osteoclast activity, and local peptidergic innervation. J Clin Periodontol 31: 596-603, 2004.
21. Nishida E, Hara Y, Kaneko T, Ikeda Y, Ukai T and Kato I: Bone resorption and local interleukin-1alpha and interleukin-1beta synthesis induced by Actinobacillus actinomycetemcomitans and Porphyromonas gingivalis lipopolysaccharide. J Periodontal Res 36: 1-8, 2001.
22. Marchesan J, Girnary MS, Jing L, Miao MZ, Zhang S, Sun L, Morelli T, Schoenfisch MH, Inohara N, Offenbacher S and Jiao Y: An experimental murine model to study periodontitis. Nat Protoc 13: 2247-2267, 2018.
23. Kimura S, Nagai A, Onitsuka T, Koga T, Fujiwara T, Kaya H and Hamada S: Induction of experimental periodontitis in mice with Porphyromonas gingivalis-adhered ligatures. J Periodontol 71: 1167-1173, 2000.
24. Suh JS, Lee SH, Fouladian Z, Lee JY, Kim T, Kang MK, Lusis AJ, Boström KI, Kim RH and Park NH: Rosuvastatin prevents the exacerbation of atherosclerosis in ligature-induced periodontal disease mouse model. Sci Rep 10: 6383, 2020.
25. Belanger M, Rodrigues P and Progulske-Fox A: Genetic manipulation of porphyromonas gingivalis. Curr Protoc Microbiol Chapter 13: Unit13C.2, 2007.
26. Velsko IM, Chukkapalli SS, Rivera MF, Lee JY, Chen H, Zheng D, Bhattacharyya I, Gangula PR, Lucas AR and Kesavalu L: Active invasion of oral and aortic tissues by Porphyromonas gingivalis in mice causally links periodontitis and atherosclerosis. PLoS One 9: e97811, 2014.
27. Siegel SD, Amer BR, Wu C, Sawaya MR, Gosschalk JE, Clubb RT and Ton-That H: Structure and mechanism of LcpA, a phosphotransferase that mediates glycosylation of a gram-positive bacterial cell wall-anchored protein. mBio 10: pii: e01580-01518, 2019.
28. Livak KJ and Schmittgen TD: Analysis of relative gene expression data using real-time quantitative PCR and the 2(-Delta Delta C(T)) method. Methods 25: 402-408, 2001.
29. Hayashi C, Gudino CV, Gibson FC III and Genco CA: Review: Pathogen-induced inflammation at sites distant from oral infection: bacterial persistence and induction of cell-specific innate immune inflammatory pathways. Mol Oral Microbiol 25: 305-316, 2010.
30. Gibson FC III, Hong C, Chou HH, Yumoto H, Chen J, Lien E, Wong J and Genco CA: Innate immune recognition of invasive bacteria accelerates atherosclerosis in apolipoprotein E-deficient mice. Circulation 109: 2801-2806, 2004.
31. Lalla E, Lamster IB, Hofmann MA, Bucciarelli L, Jerud AP, Tucker S, Lu Y, Papapanou PN and Schmidt AM: Oral infection with a periodontal pathogen accelerates early atherosclerosis in apolipoprotein E-null mice. Arterioscler Thromb Vasc Biol 23: 1405-1411, 2003.
32. Harrington WN, Nolan J, Nedosekin DA, Smeltzer MS and Zharov VP: Real-time monitoring of bacteria clearance from blood in a murine model. Cytometry A 97: 706-712, 2020.
33. He Y, Shiotsu N, Uchida-Fukuhara Y, Guo J, Weng Y, Ikegame M, Wang Z, Ono K, Kamioka H, Torii Y, *et al*: Outer membrane vesicles derived from Porphyromonas gingivalis induced cell death with disruption of tight junctions in human lung epithelial cells. Arch Oral Biol 118: 104841, 2020.
34. O'Brien-Simpson NM, Pathirana RD, Walker GD and Reynolds EC: Porphyromonas gingivalis RgpA-Kgp proteinase-adhesin complexes penetrate gingival tissue and induce proinflammatory cytokines or apoptosis in a concentration-dependent manner. Infect Immun 77: 1246-1261, 2009.
35. Nativel B, Couret D, Giraud P, Meilhac O, d'Hellencourt CL, Viranaïcken W and Silva CRD: Porphyromonas gingivalis lipopolysaccharides act exclusively through TLR4 with a resilience between mouse and human. Sci Rep 7: 15789, 2017.
36. Maekawa T, Takahashi N, Tabeta K, Aoki Y, Miyashita H, Miyauchi S, Miyazawa H, Nakajima T and Yamazaki K: Chronic oral infection with Porphyromonas gingivalis accelerates atheroma formation by shifting the lipid profile. PLoS One 6: e20240, 2011.
37. Parameswaran N and Patial S: Tumor necrosis factor-α signaling in macrophages. Crit Rev Eukaryot Gene Expr 20: 87-103, 2010.
38. Yunna C, Mengru H, Lei W and Weidong C: Macrophage M1/M2 polarization. Eur J Pharmacol 877: 173090, 2020.
39. Rajakaruna GA, Negi M, Uchida K, Sekine M, Furukawa A, Ito T, Kobayashi D, Suzuki Y, Akashi T, Umeda M, *et al*: Localization and density of porphyromonas gingivalis and tannerella forsythia in gingival and subgingival granulation tissues affected by chronic or aggressive periodontitis. Sci Rep 8: 9507, 2018.
40. Delbosc S, Alsac JM, Journe C, Louedec L, Castier Y, Bonnaure-Mallet M, Ruimy R, Rossignol P, Bouchard P, Michel JB and Meilhac O: Porphyromonas gingivalis participates in pathogenesis of human abdominal aortic aneurysm by neutrophil activation. Proof of concept in rats. PLoS One 6: e18679, 2011.
41. Nakano K, Nemoto H, Nomura R, Inaba H, Yoshioka H, Taniguchi K, Amano A and Ooshima T: Detection of oral bacteria in cardiovascular specimens. Oral Microbiol Immunol 24: 64-68, 2009.
42. Kurihara N, Inoue Y, Iwai T, Umeda M, Huang Y and Ishikawa I: Detection and localization of periodontopathic bacteria in abdominal aortic aneurysms. Eur J Vasc Endovasc Surg 28: 553-558, 2004.
43. Shimoda A, Ueda K, Nishiumi S, Murata-Kamiya N, Mukai SA, Sawada SI, Azuma T, Hatakeyama M and Akiyoshi K: Exosomes as nanocarriers for systemic delivery of the helicobacter pylori virulence factor CagA. Sci Rep 6: 18346, 2016.
44. Takeuchi H, Sasaki N, Yamaga S, Kuboniwa M, Matsusaki M and Amano A: Porphyromonas gingivalis induces penetration of lipopolysaccharide and peptidoglycan through the gingival epithelium via degradation of junctional adhesion molecule 1. PLoS Pathog 15: e1008124, 2019.
45. Paigen B, Morrow A, Holmes PA, Mitchell D and Williams RA: Quantitative assessment of atherosclerotic lesions in mice. Atherosclerosis 68: 231-240, 1987.

46. Johnston TP, Baker JC, Hall D, Jamal S, Palmer WK and Emeson EE: Regression of poloxamer 407-induced atherosclerotic lesions in C57BL/6 mice using atorvastatin. Atherosclerosis 149: 303-313, 2000.
47. Johnston TP, Nguyen LB, Chu WA and Shefer S: Potency of select statin drugs in a new mouse model of hyperlipidemia and atherosclerosis. Int J Pharm 229: 75-86, 2001.
48. Kleemann R, Princen HM, Emeis JJ, Jukema JW, Fontijn RD, Horrevoets AJG, Kooistra T and Havekes LM: Rosuvastatin reduces atherosclerosis development beyond and independent of its plasma cholesterol-lowering effect in APOE*3-Leiden transgenic mice: Evidence for antiinflammatory effects of rosuvastatin. Circulation 108: 1368-1374, 2003.
49. Park KY and Heo TH: Combination therapy with cilostazol and pravastatin improves antiatherogenic effects in low-density lipoprotein receptor knockout mice. Cardiovasc Ther 36: e12476, 2018.
50. Potempa J, Banbula A and Travis J: Role of bacterial proteinases in matrix destruction and modulation of host responses. Periodontol 2000 24: 153-192, 2000.
51. Pavloff N, Pemberton PA, Potempa J, Chen WC, Pike RN, Prochazka V, Kiefer MC, Travis J and Barr PJ: Molecular cloning and characterization of Porphyromonas gingivalis lysine-specific gingipain. A new member of an emerging family of pathogenic bacterial cysteine proteinases. J Biol Chem 272: 1595-1600, 1997.
52. Pavloff N, Potempa J, Pike RN, Prochazka V, Kiefer MC, Travis J and Barr PJ: Molecular cloning and structural characterization of the Arg-gingipain proteinase of Porphyromonas gingivalis. Biosynthesis as a proteinase-adhesin polyprotein. J Biol Chem 270: 1007-1010, 1995.
53. Hashimoto M, Kadowaki T, Tsukuba T and Yamamoto K: Selective proteolysis of apolipoprotein B-100 by Arg-gingipain mediates atherosclerosis progression accelerated by bacterial exposure. J Biochem 140: 713-723, 2006.
54. Shepardson NE, Shankar GM and Selkoe DJ: Cholesterol level and statin use in Alzheimer disease: I. Review of epidemiological and preclinical studies. Arch Neurol 68: 1239-1244, 2011.
55. Vaya J and Schipper HM: Oxysterols, cholesterol homeostasis, and Alzheimer disease. J Neurochem 102: 1727-1737, 2007.